Optical refractive and reflective properties of resonantly absorbing media

S. A. Ahmed, M. A. Ali, K. Mitwally, and M. ElMassry

Citation: The Journal of Chemical Physics **91**, 3838 (1989); doi: 10.1063/1.456869
View online: http://dx.doi.org/10.1063/1.456869
View Table of Contents: http://scitation.aip.org/content/aip/journal/jcp/91/7?ver=pdfcov
Published by the AIP Publishing

Optical refractive and reflective properties of resonantly absorbing media

S. A. Ahmed, M. A. Ali, K. Mitwally, and M. El-Massry
Institute for Ultrafast Spectroscopy and Lasers, Department of Electrical Engineering, The City College of the City University of New York, New York, New York 10031

(Received 15 February 1989; accepted 22 June 1989)

Experiments on the reflection of polarized monochromatic laser light at the planar interface of resonantly absorbing medium and the air were made for a variety of situations, including Brewster's angle in the spectral vicinity of the resonance wavelength. An ethanolic solution of Rhodamine B, an organic laser dye luminofor with a well defined resonance absorption spectrum, was chosen as the absorbing medium. The tunable polarized output of a cw dye laser was used to provide the collimated monochromatic beam. To compare the experimental results with theory, the Fresnel reflectivity equations combined with the Kramers–Kronig relations were used to predict the reflectance in terms of the known absorption coefficient. The experimental results generally confirm the theoretical predictions.

I. INTRODUCTION

High absorption coefficients encountered in the fundamental absorption regions make transmission measurements impractical in many cases. Thus most of the work reported in the literature[1–5] involve the analysis of normal incidence reflectance data. Such data can be processed using the Kramers–Kronigs relations to yield the optical constants of an absorbing medium. In the work reported here, we examine the reflection of a polarized collimated monochromatic light beam from an absorbing medium (an organic dye solution) with a known and clearly defined resonance absorption spectrum, rather than trying to extract its absorption coefficient from the measured reflectance data. Using the tunable polarized output of a cw dye laser to provide the collimated monochromatic beam, surface reflections measurements at the planar interface of the absorbing medium and air were made for a variety of situations, including Brewster's angle in the spectral vicinity of the resonance wavelength. An ethanolic solution of Rhodamine B, an organic laser dye luminofor with a well defined resonance absorption spectrum, was chosen as the absorbing medium.

To compare the experimental results with theory, the Fresnel reflectivity equations[6] combined with the Kramers–Kronig relations[7] were used to predict the reflectance in terms of the known absorption coefficient, angle of incidence, and the wavelength.

II. THEORY

A. Background

In this section, the Fresnel reflectivity equation for the *P*-polarized beam (r_p) is expressed in a simple form and used to relate the intensity (or power) reflectance of a monochromatic collimated light beam at the planar interface between a transparent medium of incidence (usually air, $\epsilon_0 = 1$) and an absorbing medium of refraction (ϵ_1 complex) in terms of the absorption coefficient (α) of the medium, the real part (n) of the complex refractive index of the absorbing medium, the angle of incidence (ϕ), and the wavelength of the incident beam.

Then, using the Kramers–Kronig relationships, an analytical expression for the real part of the complex refractive index is obtained in terms of the absorption coefficient (i.e., the imaginary part of the complex refractive index of the absorbing medium). This result is then combined with the general reflectance expression of step 1, to predict the reflectance of an absorbing medium at any given wavelength, solely in terms of the absorption coefficient of the medium at that wavelength and the angle of incidence.

B. Reflectance in terms of n and α

The reflection of a collimated light beam is governed by the Fresnel coefficients[6]

$$r_p = \frac{\epsilon \cos\phi - (\epsilon - \sin^2\phi)^{1/2}}{\epsilon \cos\phi + (\epsilon - \sin^2\phi)^{1/2}},$$
$$r_s = \frac{\cos\phi - (\epsilon - \sin^2\phi)^{1/2}}{\cos\phi + (\epsilon - \sin^2\phi)^{1/2}}, \tag{1}$$

where p and s identify the linear polarizations parallel and perpendicular to the plane of incidence, respectively. ϕ is angle of incidence, and $\epsilon = \epsilon_1/\epsilon_0$ is the complex ratio of dielectric constants of the two media defined as

$$\epsilon = \epsilon' + j\epsilon'' \tag{2}$$

and rewritten for algebraic convenience as

$$\epsilon = a + jb$$

using the following abbreviations:

$$Q = a - \sin^2\phi, \qquad |U| = (Q^2 + b^2)^{1/2},$$
$$\theta = \tan^{-1}(b/Q), \quad Z = \sqrt{|U|}/\cos\phi$$

the reflectance for the P polarized beam, $\Re_p = r_p r_p^*$, can be expressed in the form

$$\Re_p = \frac{a^2 + b^2 + Z^2 - 2|Z\{a\cos(\theta/2) + b\sin(\theta/2)\}|}{a^2 + b^2 + Z^2 + 2|Z\{a\cos(\theta/2) + b\sin(\theta/2)\}|}. \tag{3}$$

We next relate the real and imaginary quantities a and b to the absorption coefficient of the medium. The complex refractive index, N, is defined by: $N = n + jk$, where the imaginary part k is related to the absorption coefficient α by

 0021-9606/89/193838-08$02.10

$$k = \frac{c}{2\omega}\alpha(\omega), \tag{4}$$

where c is the speed of light in free space and ω is the angular frequency.

The complex refractive index N is also related to the dielectric constant of the medium by the relation:

$$N^2 = \varepsilon = \{n^2 - k^2\} + j2nk = a + jb \tag{5}$$

combining Eqs. (2), (4), and (5) gives

$$a = n^2 - \frac{c^2}{4\omega^2}\alpha^2(\omega), \quad b = n\frac{c}{\omega}\alpha(\omega). \tag{6}$$

This means that all the terms in Eq. (3) are now available in terms of n and α (as well as ω, c, and ϕ).

C. Reflectance in terms of α

We now turn to the second part of the problem to find $n(\omega)$ in terms of the absorption coefficient $\{\alpha(\omega)\}$, so that the solution of Eq. (3) can be obtained in terms of the absorption coefficient only.

Since the imaginary part $\{k(\omega)\}$ of the complex refractive index is given by Eq. (4) in terms of α and ω, using the Kramers–Kronig relations, the real part $\{n(\omega)\}$ can also be determined in terms of α and ω within an arbitrary constant (n_1) which can be determined from the specific physical conditions. The Kramers–Kronig relation for the real part $n(\omega)$ is given by[8]

$$n(\omega') = n_1 + \frac{1}{\pi}\text{P.V.}\int_{-\infty}^{\infty}\frac{k(\omega)}{(\omega - \omega')}d\omega, \tag{7}$$

where P.V. means the Cauchy principal value. It is important to stress the generality of the relation of Eq. (7). It requires only boundedness and causality.[9] These conditions are necessarily fulfilled by virtue of the fact that the polarization of a wave cannot antecede the arrival of the disturbing electric field that produces it.[10]

Rewriting Eq. (7) in terms of α [Eq. (4)] gives

$$n(\omega') = n_1 + \frac{c}{2\pi}\text{P.V.}\int_{-\infty}^{\infty}\frac{\alpha(\omega)}{\omega(\omega - \omega')}d\omega. \tag{8}$$

To obtain reflectance in the vicinity of the absorption resonance, using Eq. (3), it is first necessary to evaluate the integration of Eq. (8) over the spectral range of interest, and then substitute the results into Eq. (3). To evaluate the integration in Eq. (8), two possible approaches could be used. The first would be to carry out a numerical integration using the actual measured absorption line shape (Fig. 1).

The second approach is to assume a Lorentzian approximation for the absorption line shape in the vicinity of the peak, and to analytically integrate Eq. (8) to get an analytical expression for $n(\omega)$. For this approach, we assume a Lorentzian function for the absorption coefficient $\alpha(\omega)$, given by:

$$\alpha(\omega) = \frac{\alpha(\omega_0)\gamma^2}{(\omega - \omega_0)^2 + \gamma^2}, \tag{9}$$

where $\gamma = (\Delta\omega/2)$, and $\alpha(\omega_0)$ is the absorption coefficient at resonance. Substituting Eq. (9) into Eq. (8) and carrying out the integration we get (see the Appendix):

$$n(\omega) = n_1 + \left\{\frac{c(\omega_0^2 - \omega\omega_0 - \gamma^2)}{2\gamma(\omega_0^2 + \gamma^2)}\right\}\alpha(\omega). \tag{10}$$

At this point, it should be noted that as long as $\Delta\omega \ll \omega_0$, the evaluation of the integral in Eq. (8), depends primarily on the absorption and hence dispersion in the immediate vicinity of the resonance center.[9] The successful use of the Kramers–Kronig relations, depends, in their contest, in the fact that negligible error results from a lack of knowledge of frequency spectrum remote from the point of interest (in our

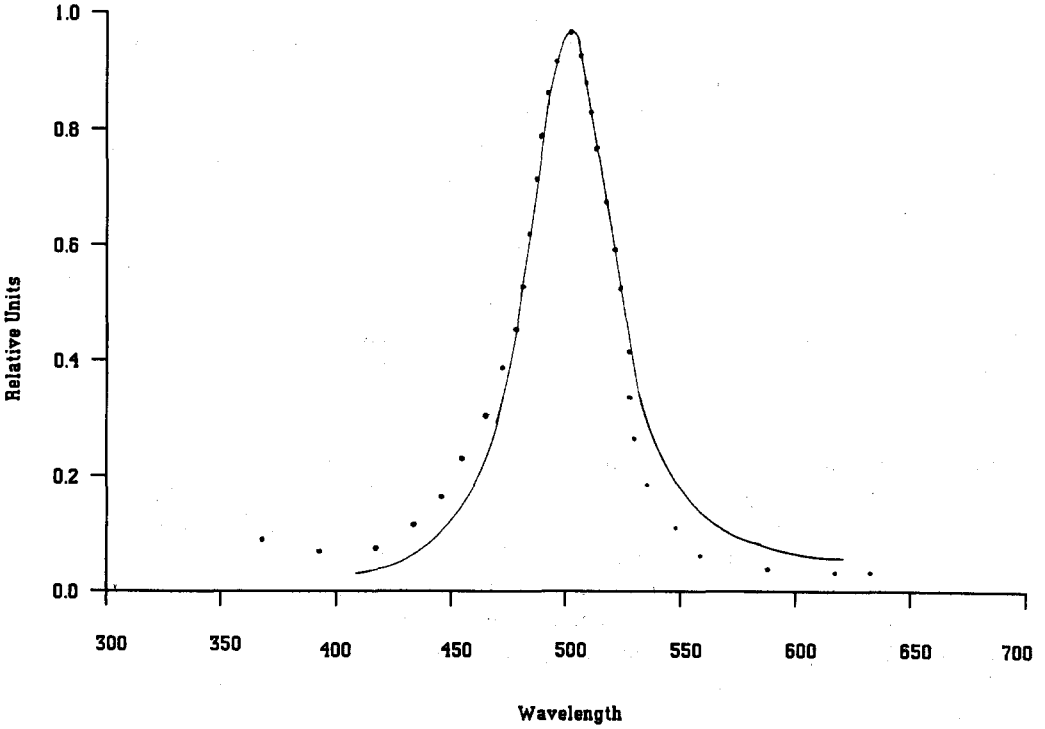

FIG. 1. Absorption spectrum of Rhodamine B in Ethanol: (—) Lorentzian, (●) Experimental.

case, outside the vicinity of resonance frquency).[11] To integrate Eq. (8) using the Lorentzian approximation, we use actual measured values for magnitude of peak absorption, $\alpha(\omega_0)$, peak frequency, ω_0, and the linewidth, 2γ. Since in the vicinity of resonance, the actual absorption line shape is almost Lorentzian, one is led to the conclusion that the use of a Lorentzian line shape in Eq. (8) can be expected to give almost the same results as the numerical integration in the vicinity of resonance.

For the Lorentzian approximation, combining Eqs. (6) and (10) into Eq. (3) gives the final expression for reflectance for any absorbing medium in terms of basic information about its absorption coefficient. This expression is Eq. (3), repeated here for convenience:

$$\Re_p = \frac{a^2 + b^2 + Z^2 - 2|Z\{a\cos(\theta/2) + b\sin(\theta/2)\}|}{a^2 + b^2 + Z^2 + 2|Z\{a\cos(\theta/2) + b\sin(\theta/2)\}|}, \tag{3}$$

where however, now

$$a = \left\{ n_1 + \left[\frac{c(\omega_0^2 - \omega\omega_0 - \gamma^2)}{2\gamma(\omega_0^2 + \gamma^2)} \right] \alpha(\omega) \right\}^2 - \left\{ \frac{c^2}{4\omega^2} \alpha^2(\omega) \right\},$$

$$b = \left\{ n_1 + \left[\frac{c(\omega_0^2 - \omega\omega_0 - \gamma^2)}{2\gamma(\omega_0^2 + \gamma^2)} \right] \alpha(\omega) \right\} \frac{c}{\omega} \alpha(\omega),$$

and Z and θ are as previously defined in terms of a, b, and ϕ.

Predictions for reflectance using the actual absorption line shape (numerical integration) and the Lorentzian approximation are compared with each other and with experimental measurements, in the following section.

III. EXPERIMENTAL

The solution of Rhodamine B in ethanol was selected as the lossy refractive medium from which reflections of collimated light beams are measured at the air medium interface. Rhodamine B was selected because it has a well defined absorption resonance in the green–yellow spectral region (Fig.1) which is readily accessible to the cw organic dye laser used to provide the tunable collimated light beam. Furthermore, the absorption spectrum, in the vicinity of the resonance, is reasonably close to the Lorentzian shape assumed in Sec. II above to facilitate the evaluation and the numerical calculations needed to make theoretical predictions (see comparison in Fig. 1). Actually measured values for magnitude of peak absorption, peak wavelength, and the linewidth, were those used in the Lorentzian approximation to evaluate theoretical expressions.

The actual experimental set up is relatively straight forward. A polarized collimated light beam is obtained from a tunable cw dye laser. By appropriate geometric arrangements of mirrors, the angle of incidence of the laser beam on the dye solution surface can be varied, and the incident and reflected powers at the dye-air interface measured using pv detectors. To increase sensitivity and accuracy, a phase lock loop amplifier was used in conjunction with the detectors. Measurements and comparisons with theoretical predictions were made for the "p" polarized ray only, since results for the "s" polarization are expected to differ only in some details, that would not be expected to add to the understanding of the process or the confirmation of the models used.

IV. COMPARISONS OF THEORETICAL PREDICTIONS AND EXPERIMENTAL RESULTS

The following parameters were measured experimentally and used in theoretical calculations:

i) an absorption peak (λ_0) at 552 nm,

ii) a line width ($\Delta\lambda$) of approximately 40 nm,

iii) a peak absorption coefficient, α (ω_0) of 5×10^4 cm^{-1}.

The arbitrary constant (n_1) in Eq. (10) is assigned a value of 1.364, which is the refractive index of the solvent (ethanol) used in our experiment. This is understood by assuming a zero value to the absorption coefficient (α) in Eq. (10), thus the medium is now lossless and its refractive index is reduced to the refractive index of the transparent solvent.

Experimental results and their theoretical comparisons are divided into three different sets.

A. Set I

Experimental measurements were carried out to determine and measure the reflectance as a function of wavelength at three different angles 29°, 54°, and 75°, respectively. As will be seen later, the significance of choosing the angle 54° is that this is the angle of minimum reflection, or pseudo-Brewster angle (PB), at the resonance frequency. It is also close to the theoretically calculated and experimentally measured value of Brewster's angle for the ethanol solvent alone.

Figures 2, 3, and 4 show the experimental results along with theoretical predictions. The theoretical predictions are made: (i) using the Lorentzian approximation evaluated with actual measured values for magnitude of peak absorption, peak wavelength, and the linewidth, and (ii) by carrying out numerical integrations using the actual absorption line shape.

The theoretical predictions are carried out and compared with each other and with the experimental results of this set in Figs. 2, 3, and 4. These comparisons show a good agreement between the Lorentzian approximation and the numerical integration using the actual absorption line shape. Off resonance, where the difference between the Lorentzian line shape and the actual line shape is clear, α has a small value, and R_p values are in general less sensitive to variations in α. In order to more readily appreciate the relationship between the absorption and the reflectance curves, the theoretically assumed (Lorentzian) absorption spectrum is also shown, with, however, the same peak and linewidth as are measured experimentally.

When the angle of incidence is 29°, the maxima for the reflectance is shifted towards longer wavelengths, when it is 75° the maxima for the reflectance is shifted towards shorter wavelengths, while there is no shift at all when the angle of incidence is 54° (PB angle at resonance). It is also interesting that the closest fit between theoretical predictions and experimental results is obtained when the angle of incidence is the PB angle at resonance.

With the adequateness of the Lorentzian approximation thus established, the remaining figures show only theoretical

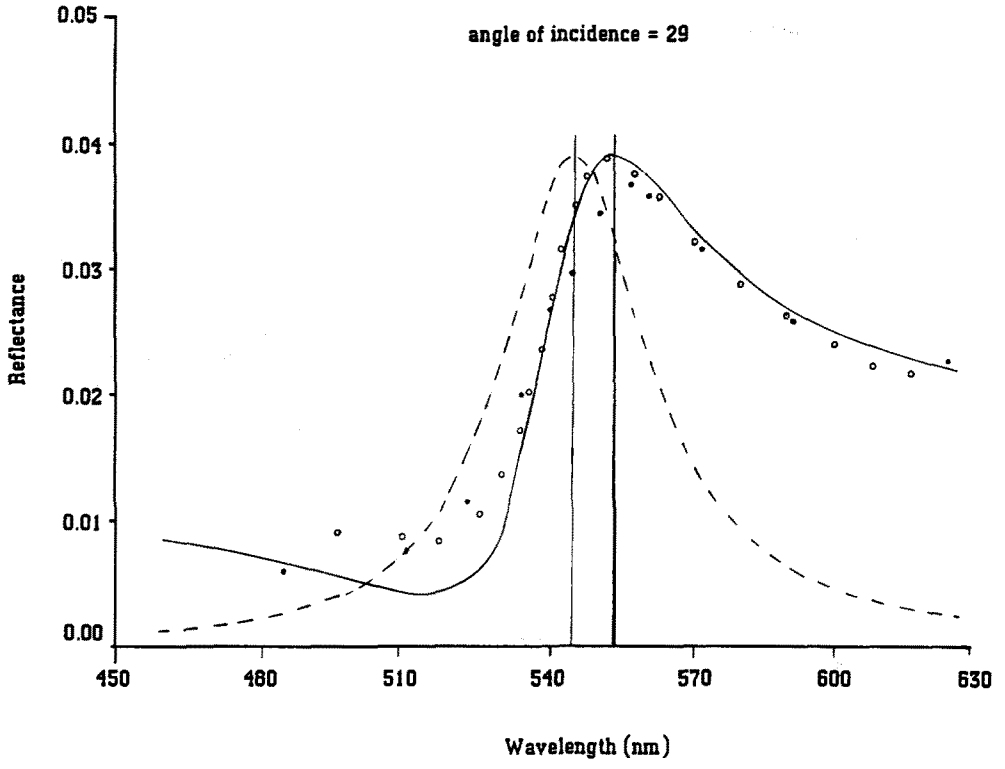

FIG. 2. Reflectance R_p vs λ for Rh B solution at angle of incidence $\phi = 29°$: (—) theoretical (Lorentzian), (○) theoretical (actual lineshape), (●) experimental, (---) absorption spectrum.

predictions based on the Lorentzian approximation, along with results of experimental measurements.

B. Set II

Theoretical predictions using the Lorentzian approximation and experimental measurements were carried out to predict and measure the reflectance as a function of the angle of incidence for three different wavelengths, 514, 552, and 580 nm, respectively. Figures 5 and 6 show the theoretical predictions and the corresponding experimental measurements for the reflectance (R_p) vs the angle of incidence (ϕ) at these wavelengths, respectively. It is seen that there is no angle which corresponds to exactly zero reflection. The angle at which R_p has a minimum value is called the pseudo–Brewster (PB) angle.

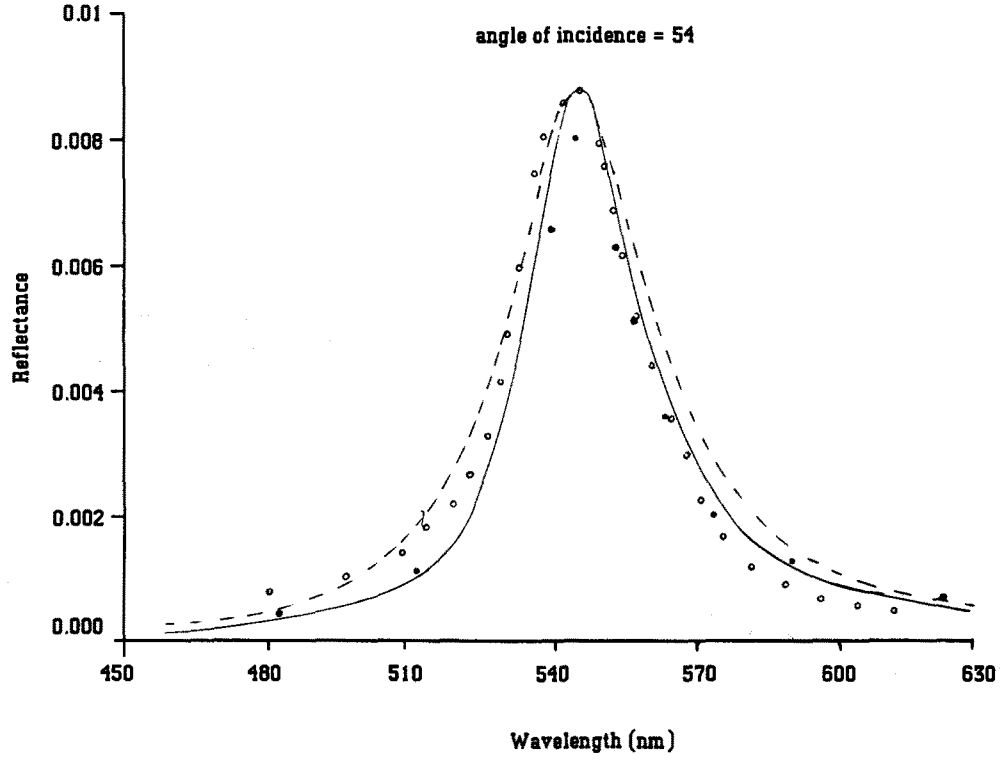

FIG. 3. Reflectance R_p vs λ for Rh B solution at angle of incidence $\phi = 54°$:(—) theoretical (Lorentzian), (○) theoretical (actual lineshape), (●) experimental, (---) absorption spectrum.

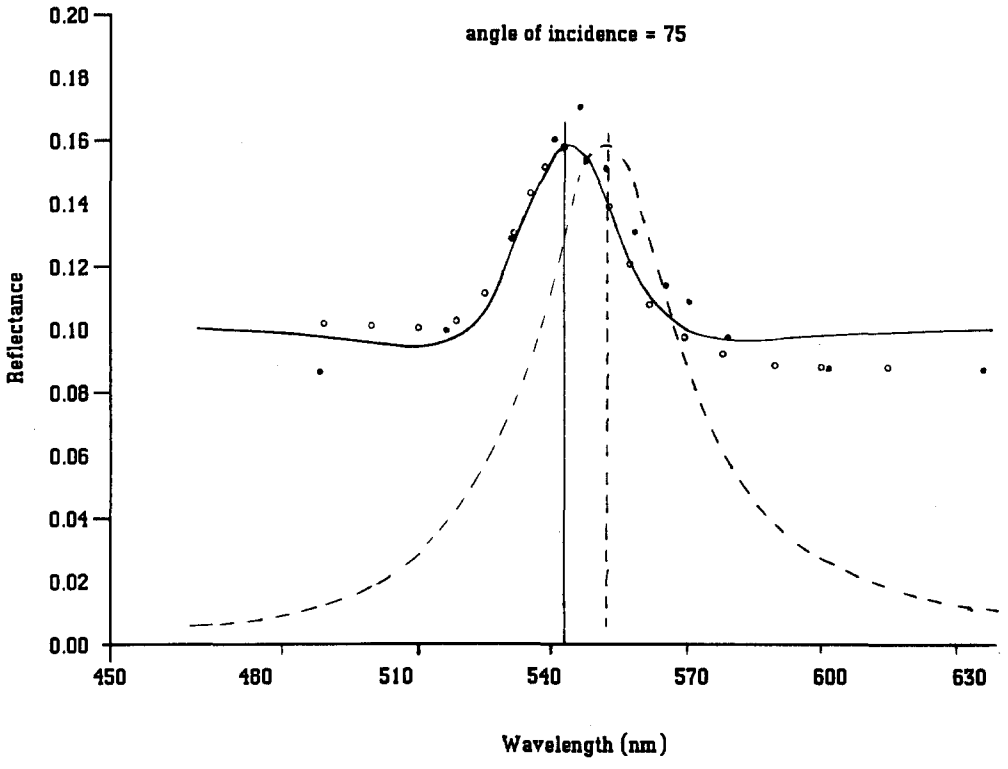

FIG. 4. Reflectance R_p vs λ for Rh B solution at angle of incidence $\phi = 75°$: (—) theoretical (Lorentzian), (○) theoretical (actual lineshape), (●) experimental, (---) absorption spectrum.

From Fig. 5 (theoretical result), we have at $\lambda = 514$ nm, ϕ_{PB} (incident angle of minimum reflectance) $= 50°$, and the corresponding reflectance $Rp = 0.0005$. At $\lambda = 552$ nm, $\phi_{PB} = 53.7°$, and $Rp = 0.01$. At $\lambda = 580$ nm, $\phi_{PB} = 57.5°$, and $Rp = 0.001$.

Again, there is reasonably good agreement between theoretical predictions and experimental results (Fig. 6) particularly at the resonance wavelength (552 nm). Figures 5 is redrawn in Fig. 7, with a different scale, to more readily distinguish between the data.

C. Set III

Theoretical predictions again using the Lorentzian approximation and experimental measurements were carried out to predict and measure the pseudo-Brewster angles and

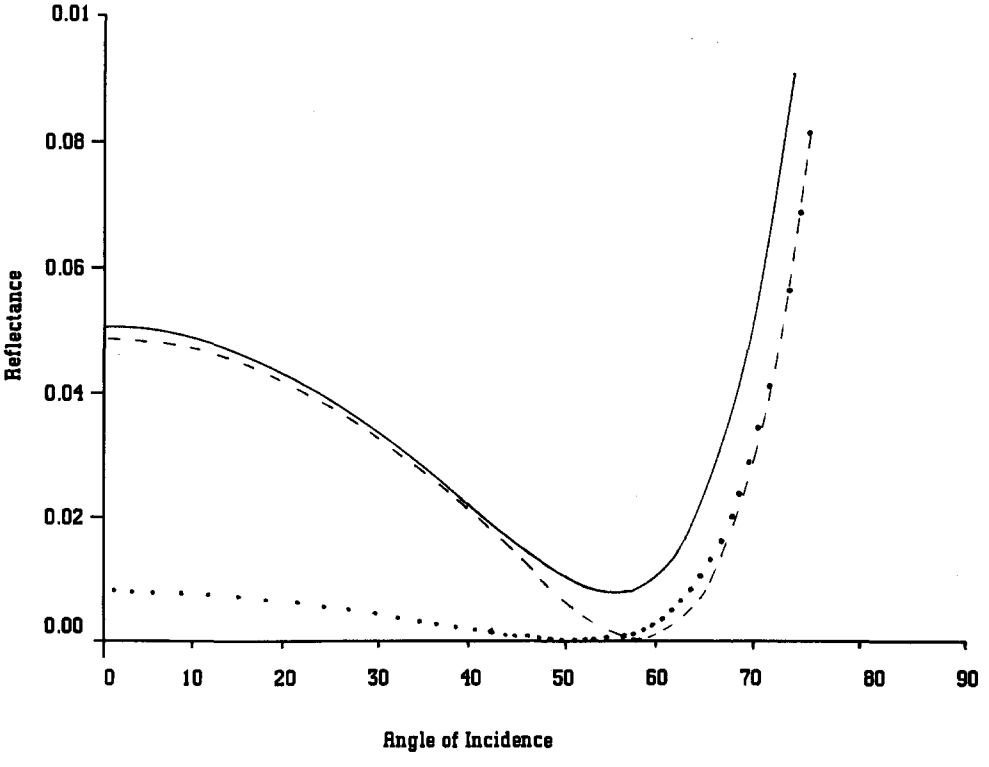

FIG. 5. Theoretical predictions of reflectance R_p vs angle of incidence ϕ at wavelengths $\lambda = 514$, 552, and 580 nm: (—) 552 nm, (---) 580 nm, (●) 514 nm.

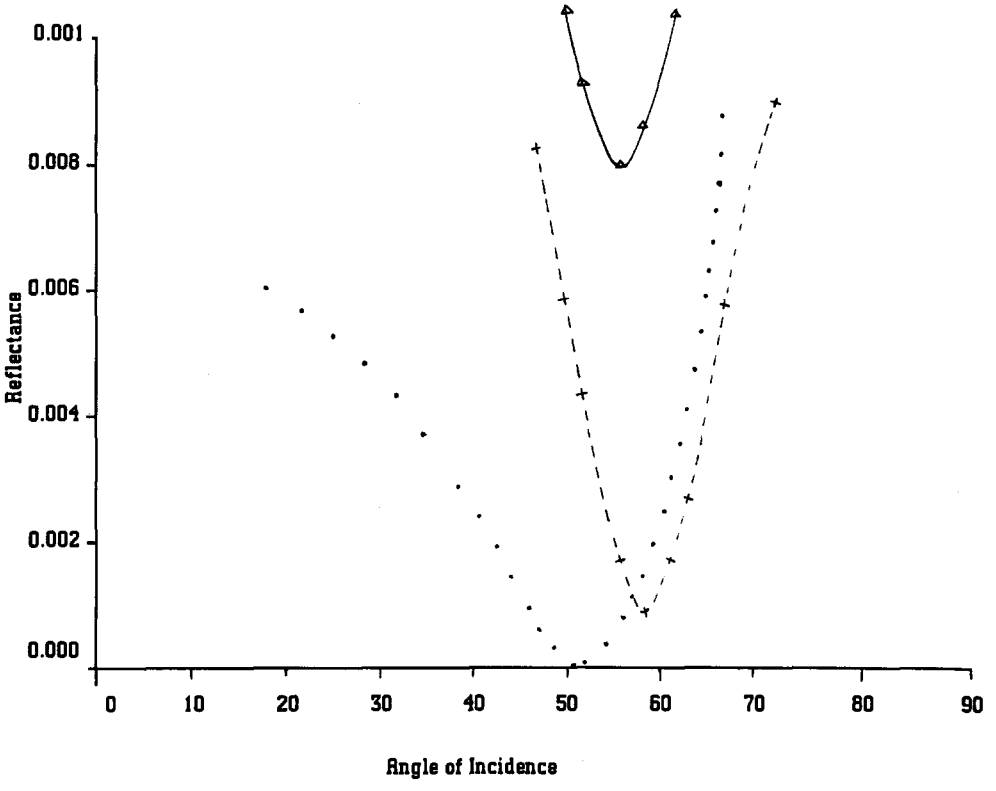

FIG. 6. Experimental measurements of reflectance R_p vs angle of incidence ϕ at wavelengths $\lambda = 514$, 552, and 580 nm, (△) 552 nm, (+) 580 nm, (●) 514 nm.

the reflectance corresponding to these angles vs λ. It would be emphasized that, for any given λ, the PB angles were not determined by setting Rp in Eq. (3) equal to zero and then finding the corresponding angle, since such a solution does not exist. Instead, for a given λ, R_p was calculated for all ϕ's from $\phi = 0°$–$90°$, with increments of 0.01°, and the angle with corresponding to the minimum reflectance is considered as the PB angle for that λ.

Figure 8 shows the theoretical predictions and the experimental measurements for ϕ_{PB} vs λ. Figure 9 shows the

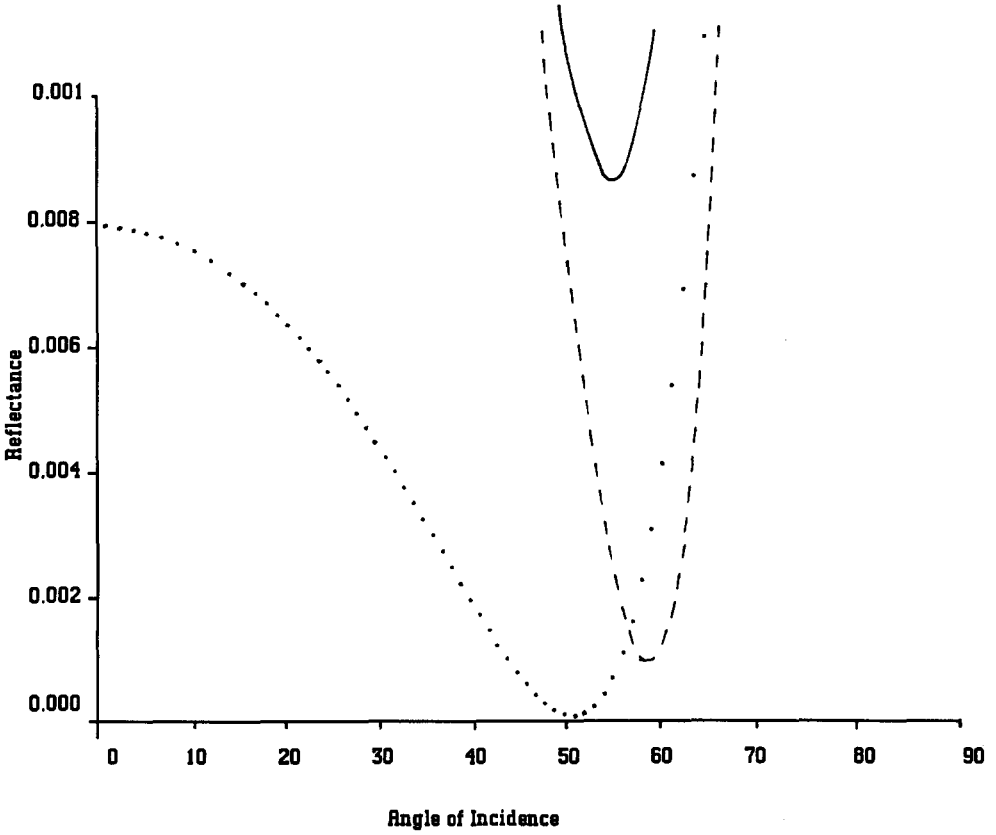

FIG. 7. Expansion of Fig. 5 with the scale used in Fig. 6 to more readily distinguish between the data.

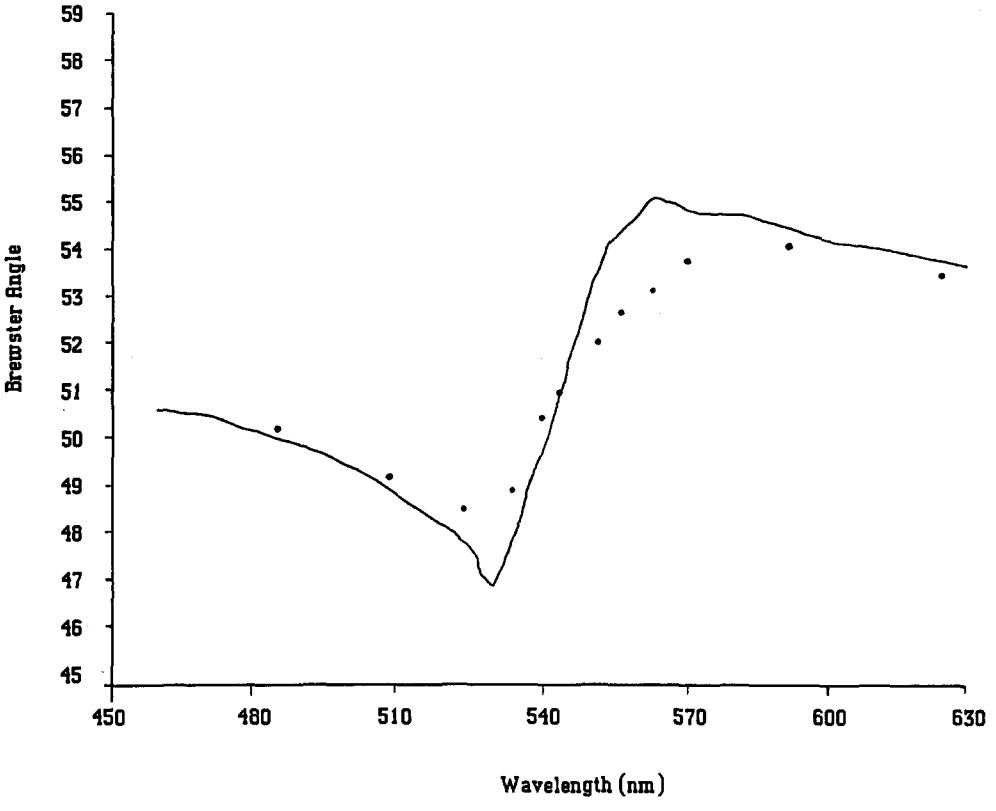

FIG. 8. Pseudo-Brewster angle ϕ_{PB} vs λ: (—) theoretical and (●) experimental.

theoretical predictions and the experimental measurements for reflectance at the PB angles vs λ, showing a good fit between experimental and theoretical results and with the reflectance at the PB angles tracking the absorption.

V. CONCLUSION

We have reported experimental work on surface reflections measurements at the planar interface of resonantly absorbing medium and the air for a variety of situations. An ethanolic solution of Rhodamine B, an organic laser dye luminofor with a well defined resonance absorption spectrum, was used as the absorbing medium. It was found that the maxima for reflectance coincide with the maxima for absorption when the angle of incidence is equal to the PB angle at resonance frequency. However, the maxima might be shifted to longer or shorter wavelengths depending on the

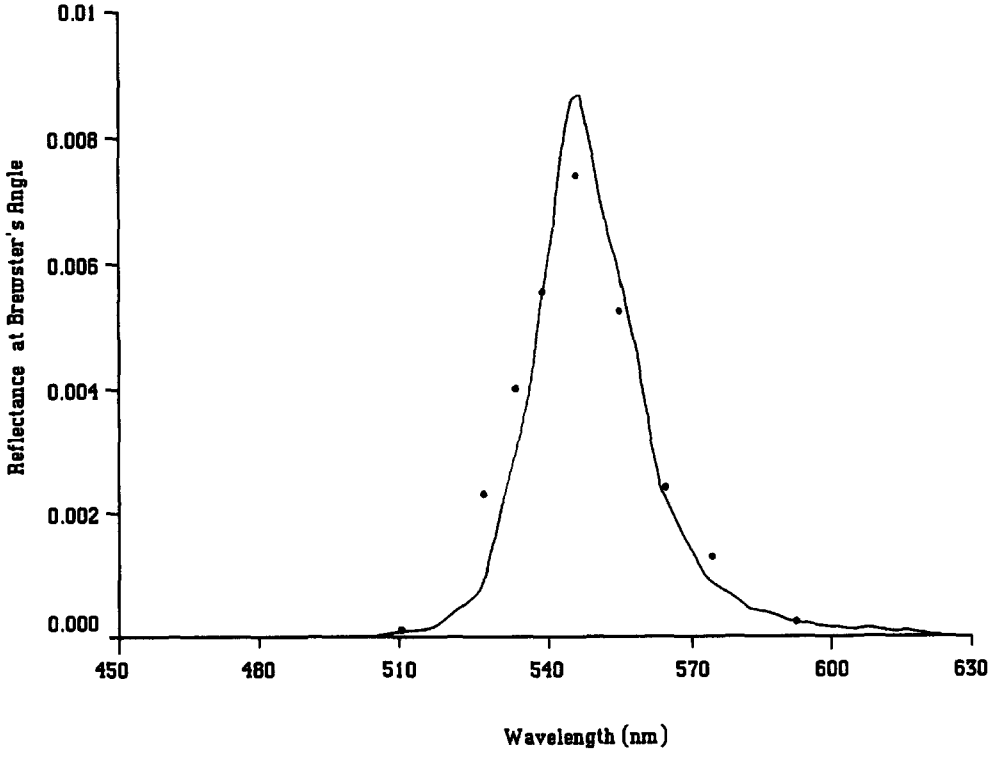

FIG. 9. Reflectance at pseudo-Brewster angles vs λ: (—) theoretical and (●) experimental.

angle of incidence. It was also found that the PB angle at resonance frequency is equal to the Brewster's angle for the solvent (lossless medium).

The Fresnel reflectivity equations combined with the Kramers–Kronig relations were used to predict the reflectance in terms of the known absorption coefficient. Our experimental results generally confirm the theoretical predictions.

APPENDIX

Consider $\oint_c F(\omega)d\omega$ where C is the closed contour shown in Fig. 10 and $F(\omega)$ is given by

$$F(\omega)=\frac{d\omega}{\omega(\omega-\omega')\{(\omega-\omega_0)^2+\gamma^2\}}, \tag{A1}$$

integrating the function $F(\omega)$ over the contour shown:

$$\oint_C F(\omega)d\omega = \int_{-R}^{-\epsilon} F(\omega)d\omega + \int_{c_1} F(\omega)d\omega + \int_{\epsilon}^{\omega'-\epsilon} F(\omega)d\omega + \int_{c_2} F(\omega)d\omega + \int_{\epsilon+\omega'}^{R} F(\omega)d\omega + \int_{c_3} F(\omega)d\omega, \tag{A2}$$

where c_1, c_2, and c_3 are the semicircular arcs of radii, ϵ, ϵ, and R. We next take the limit of Eq. (A2) as $R\to\infty$ and $\epsilon=0$.

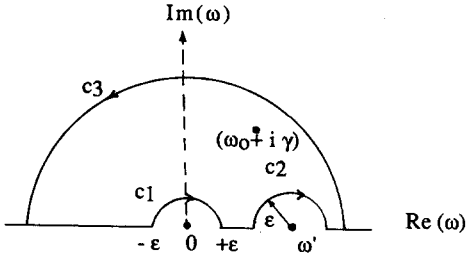

FIG. 10. The integration contour used to drive the real part (n) of the complex refractive index (N).

The integral over C_3 vanishes for $F(\infty)\to 0$ while the integral over C becomes

$$\frac{-\pi}{\gamma(\omega_0+i\gamma)(\omega'-\omega_0-i\gamma)} = \text{P.V.}\int_{-\infty}^{\infty} F(\omega)d\omega + \frac{i\pi}{\omega'(\omega_0^2+\gamma^2)} - \frac{i\pi}{\omega'\{(\omega'-\omega_0)^2+\gamma^2\}}, \tag{A3}$$

where

$$\frac{-\pi}{\gamma(\omega_0+i\gamma)(\omega'-\omega_0-i\gamma)} = 2\pi i \text{ (residue) of } F(\omega) \text{ at } \omega=\omega_0+i\gamma = \text{left-hand side of Eq. (A2)}$$

$$\frac{i\pi}{\omega'(\omega_0^2+\gamma^2)} = \int_C F(\omega)d\omega = -i\pi \text{ (residue) of } F(\omega) \text{ at } \omega=0$$

$$\frac{-i\pi}{\omega'\{(\omega'-\omega_0)^2+\gamma^2\}} = \int_{C_2} F(\omega)d\omega = -i\pi \text{ (residue) of } F(\omega) \text{ at } \omega=\omega'$$

from Eq. (A3) we get

$$\text{P.V.}\int_{-\infty}^{\infty} F(\omega)d\omega = \frac{\pi\{\omega_0^2-\omega_0\omega'-\gamma^2\}}{\gamma(\omega_0^2+\gamma^2)\{(\omega'-\omega_0)^2+\gamma^2\}}. \tag{A4}$$

[1] D. L. Greenaway and G. Harbeke, *Optical Properties and Band Structure of Semiconductors* (Pergamon, New York, 1968).
[2] H. R. Philipp and E. A. Taft, Phys. Rev. **113**, 1002 (1959).
[3] E. D. Palik, *Handbook of Optical Constants of Solids* (Academic, New York, 1985).
[4] S. P. F. Humphreys-Owen, Proc. Phys. Soc. (London) **77**, 949 (1961).
[5] D. E. Aspnes and A. A. Studna, Phys. Rev. B **27**, 985 (1983).
[6] R. M. A. Azzam and A. M. El-Saba, Appl. Opt. **27**, 4034 (1988).
[7] A. Yariv, *Quantum Electronics* (Wiley, New York, 1975).
[8] B. S. Gourary, J. Appl. Phys. **28**, 3 (1957).
[9] J. H. Van Vleck, Rl Report No. 735, 1945.
[10] H. A. Kramers, Atti Congresso Internazionale Fisici Como **2**, 545 (1927).
[11] F. C. Jahoda, Phys. Rev. **107**, 1261 (1957).